ELSEVIER

Contents lists available at ScienceDirect

International Journal of Biological Macromolecules

journal homepage: www.elsevier.com/locate/ijbiomac





Sulfated fuco-manno-glucuronogalactan alleviates pancreatic beta cell senescence via PI3K/AKT/FoxO1 pathway

Wenjing Zhang ^{a,1}, Nan Wu ^{a,1}, Hong Wang ^a, Genxiang Mao ^c, Xiaojun Yan ^d, Fuming Zhang ^e, Robert J. Linhardt ^{e,f}, Weihua Jin ^{b,*}, Jiaqiang Zhou ^{a,*}

- ^a Department of Endocrinology and Metabolism, Sir Run Run Shaw Hospital, Zhejiang University School of Medicine, Hangzhou 310016, China
- ^b College of Biotechnology and Bioengineering, Zhejiang University of Technology, Hangzhou 310014, China
- ^c Zhejiang Provincial Key Lab of Geriatrics, Department of Geriatrics, Zhejiang Hospital, Hangzhou 310013, China
- ^d Marine Science and Technical College, Zhejiang Ocean University, Zhoushan 316022, China
- e Department of Chemical and Biological Engineering, Center for Biotechnology and Interdisciplinary Studies, Rensselaer Polytechnic Institute, Troy, NY 12180, USA
- f Department of Biological Science, Departments of Chemistry and Chemical Biology and Biomedical Engineering, Center for Biotechnology and Interdisciplinary Studies, Rensselaer Polytechnic Institute, Troy, NY 12180, USA

ARTICLE INFO

Keywords: Sulfated fuco-manno-glucuronogalactan Pancreatic beta cell senescence PI3K/AKT/FoxO1

ABSTRACT

Appearance of senescent beta cells in the pancreas leads to the onset of type 2 diabetes (T2D). The structural analysis of a sulfated fuco-manno-glucuronogalactan (SFGG) indicated SFGG had the backbones of interspersing 1, 3-linked β -D-GlcpA residues, 1, 4-linked α -D-Galp residues, and alternating 1, 2-linked α -D-Manp residues and 1, 4-linked β -D-GlcpA residues, sulfated at C6 of Man residues, C2/C3/C4 of Fuc residues and C3/C6 of Gal residues, and branched at C3 of Man residues. SFGG effectively alleviated senescence-related phenotypes in vitro and in vivo, including cell cycle, senescence-associated β -galactosidase, DNA damage and senescence-associated secretory phenotype (SASP) -associated cytokines and hall markers of senescence. SFGG also alleviated beta cell dysfunction in insulin synthesis and glucose-stimulated insulin secretion. Mechanistically, SFGG attenuated senescence and improved beta cell function via PI3K/AKT/FoxO1 signaling pathway. Therefore, SFGG could be used for beta cell senescence treatment and alleviation of the progression of T2D.

1. Introduction

In 2019, the global diabetes prevalence was estimated to be 463 million people, and the number was projected to rise to 578 million by 2030 [1]. Diabetes mellitus (DM) is a chronic disease represented by relative or absolute insulin insufficiency associated with pancreatic beta cells, leading to elevation of blood sugar levels, which is related to many metabolic diseases [2,3]. Evidence indicates clearly that cell dysfunction induced by glucotoxicity in pancreatic beta cells relates to the pathogenesis of type 2 diabetes (T2D) [4]. Old age is also contributed to the development of T2D [5–8]. Both glucotoxicity and aging contribute to the diabetic microenvironment that promotes beta cell senescence [6,9].

The senescent beta cells downregulate the expression of key genes related to their function and identity, contributing to loss of function, cellular identity and worsening metabolic profile [10]. Cellular senescence is defined as a state of cell cycle arrest, the chromatin change and

protein synthesis increased including secreting massive amounts of senescence-associated secretory phenotype (SASP) factors [10-12]. Li et al. found the thioredoxin-interacting protein (TXNIP) exacerbated pancreatic beta cell senescence and age-related dysfunction by inducing cell cycle arrest through the p38-p16/p21-CDK-Rb pathway in TXNIP and C57BL/6 mice [13]. The SASP was a primary mediator of the detrimental effects of senescent cells. SASP could trigger inflammatory responses, disrupted the tissue microenvironment and homeostasis by the secretion of extra cellular matrix components, recruitment of immune cells, or affecting the fate of other cells in the tissue [14]. Transcriptional analyses showed the SASP factors are produced and secreted by senescent beta cells, and the senescent beta cells might lead to senescence of neighboring beta cells via secretion of SASP in a paracrine action [6]. The expression of senescence markers ($p16^{\text{INK4a}}$, $p21^{\text{Cip1}}$) and the SASP (Il6, Il1a, Tnf, Ccl2, and Cxcl1) were upregulated in SA-β-Gal⁺ pancreatic beta cells and beta cell markers (Ins1, Pdx1, Mafa, Nkx6.1,

E-mail addresses: jinweihua@zjut.edu.cn (W. Jin), zjq8866@zju.edu.cn (J. Zhou).

¹ Contributed equally.

^{*} Corresponding authors.

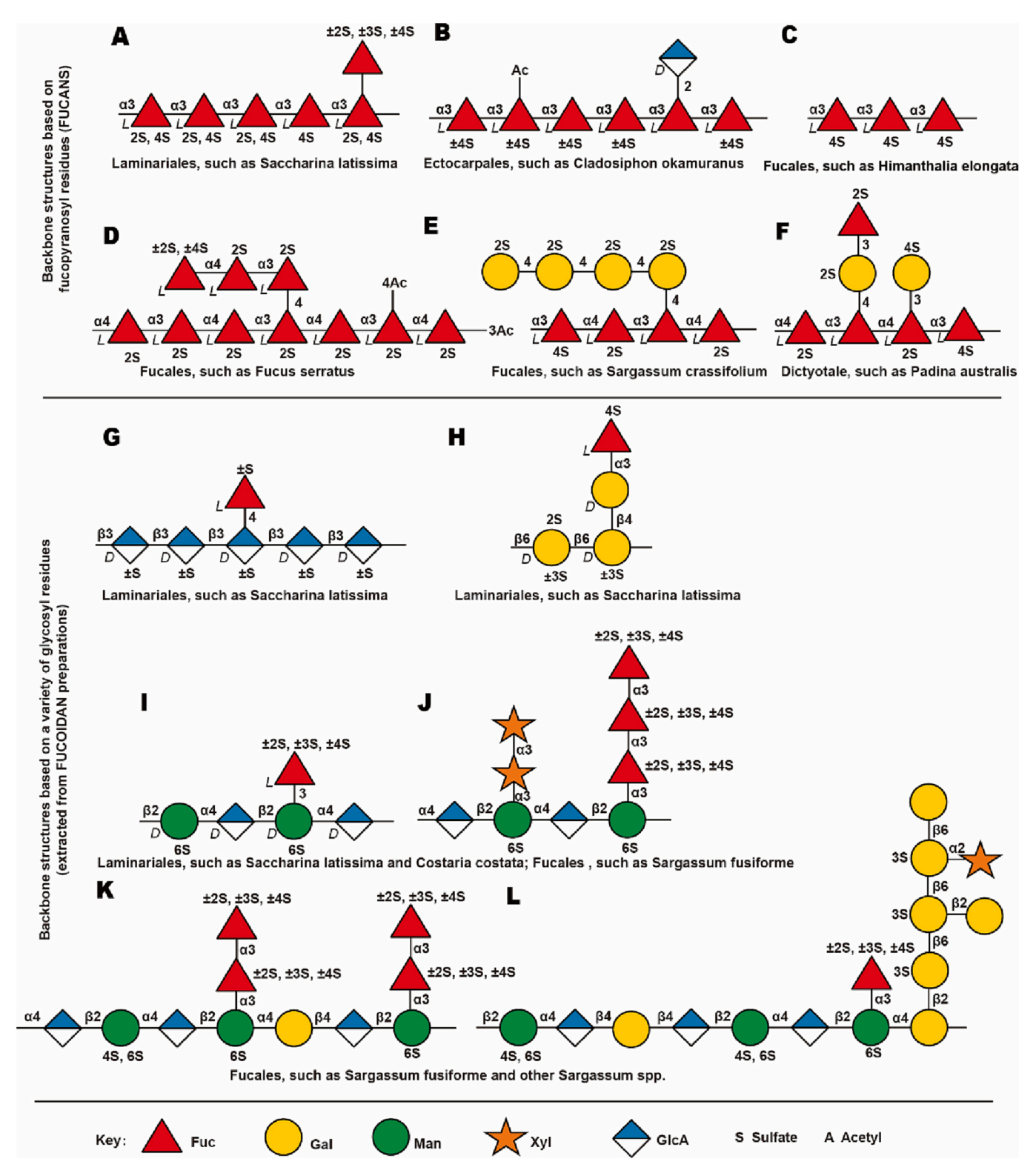


Fig. 1. The structural features of some fucoidans from brown algae. (A-F) backbone structures based on fucopyranosyl residues, such as sulfated fucan, sulfated galactofucan and sulfated glucuronofucan; (G-L) backbone structures based on a variety of glycosyl residues, containing sulfated fucogalactan, sulfated fucoglucuronan, sulfated fucoglucuronomannan and sulfated xylo-fucoglucuronomannans. [33].

and *Neurod1*) was the downregulated, and this up-regulation of genes that were usually suppressed in SA- β -Gal $^-$ beta cells [6]. These changes in senescent beta cells result in the pathogenesis of DM.

Currently, 'senolytic' drugs that kill senescent cells or inhibit the secretion of SASP factors are the main approaches used to treat T2D [15]. Rapamycin and related agents can prolong the lifespan of patients

and decrease the incidence of associated conditions such as heart failure, cancer, and immune dysfunction [15]. Metformin can inhibit the SASP by interfering with IKK/NF- κ B activation [16,17]. ABT263 (inhibitor of the Bcl-2 family) has been shown to alleviate cell senescence, improve glucose metabolism and beta cell function, downregulate the expression of markers of aging and senescence and inhibit the secretion of SASP

factors in INK-ATTAC model [6]. Although drugs that target beta cell senescence have emerged, the agents that are currently available do not achieve satisfactory results and new drugs that also promote beta cells regeneration are urgently required.

Fucoidan, a heparin-like sulfated polysaccharide found widely in brown seaweeds, has been demonstrated to have numerous biological activities, including anti-inflammatory, anti-viral, anti-senescence, antitumor, antioxidant, anti-hyperlipidemia, regulating metabolic disorders, enhancing central nervous system and anti-tumor effects [18-25]. Fucoidan from Sargassum fusiforme was found to activate the NRF2 pathway to alleviate obesity and insulin resistance [26]. Fucoidan also reduced pancreatic beta cell death and enhanced insulin synthesis via the SIRT1/PDX1/GLP1-R pathway in streptozotocin-induced mouse model of mice [27]. In addition, Jiang et al. indicated the fucoidan protects beta cell function through the cAMP signaling pathway [28]. However, reports on the anti-senescence activity of fucoidan are rare. Min et al. reported that fucoidan reduce the viability and induced apoptosis of hepatocellular carcinoma cells and prevented senescence of normal liver cells [29]. Lee et al. found that pretreatment with fucoidan reversed senescence of endothelial colony-forming cells (ECFCs) through the FAK, AKT, and ERK signaling pathways [30]. Fucoidan also reversed the mesenchymal stem cell (MSC) senescence induced by pcresol through regulation of cell cycle-associated proteins and cellular prion proteins [31]. Moreover, fucoidan inhibited the formation of senescence-associated heterochromatin foci and regulated the expression of senescence-associated proteins p21 and p16. A Sargassum fusiforme-derived fucoidan SP2 was also shown to activate the NRF2mediated antioxidant signaling pathway during the aging process [32]. This information led to the hypothesis that prevention of pancreatic beta cell senescence by fucoidans is a promising strategy for the treatment of type 2 diabetes.

Fucoidans are complicated chemical structures containing fucose, galactose, mannose, rhamnose, glucose and uronic acid, with biological activities that may vary depending on the species of brown algae, harvest time and location and methods used for extraction. According to the previous review [33], the structures of fucoidans (also named as fucosecontaining sulfated polysaccharides, FCSPs) were summarized in Fig. 1. They can be divided into two types: 1) backbone structures based on fucopyranosyl residues, such as sulfated fucan, sulfated galactofucan and sulfated glucuronofucan and 2) backbone structures based on a variety of glycosyl residues, containing sulfated fucogalactan, sulfated fucoglucuronan, sulfated fucoglucuronomannan and sulfated xylofucoglucuronomannans.

In this study, we prepared a fuco-manno-glucuronogalactan (SFGG) derived from *Saccharina japonica*. Based on the anti-senescence activity of fucoidan, we speculated that SFGG could attenuate pancreatic beta cell senescence and treat T2D. Therefore, we evaluated SFGG's effects on pancreatic beta cells in senescent MIN6 cells and mouse model. Our work provides the potential drug for beta cell senescence and inhibition of the progression of T2D.

2. Materials and methods

2.1. Materials

The MIN6 pancreatic beta cell line was cultured in high glucose Dulbecco's modified Eagle's medium (DMEM), containing 0.05 % 2-mercaptoethanol (Sigma-Aldrich, Bioreagent, St. Louis, MO, USA), 15 % fetal bovine serum for embryonic stem cells (ES-FBS; Vistech, New Zealand), 100 U/mL penicillin and 100 μ g/mL streptomycin (Gibco, Carlsbad, CA, USA) at 37 °C in a humidified atmosphere under 5 % CO₂. Hydrogen peroxide (H₂O₂) was purchased from Sigma-Aldrich (Sigma-Aldrich, USA).

2.2. Preparation and analysis of SFGG

Fucoidan was prepared as previously described [34,35]. Briefly, fucoidan (1 g) was dissolved in 0.1 M hydrochloric acid (HCl) and stirred for 2 h at 80 °C. The degradation solution was neutralized, concentrated, and precipitated using ethanol. The precipitate was re-dissolved and degraded using 0.5 M HCl. The degradation solution was neutralized, concentrated, and precipitated using ethanol. The precipitate was re-dissolved and further purified on a Bio-Gel P-10 column (2.6 \times 100 cm) eluted with 0.2 M NH4HCO3 to obtain SFGG. SFGG was refluxed in 0.1 M sulfuric acid for 4 h. The solution was then neutralized, centrifuged, concentrated and ultrafiltered by using a Ultracel 3 kDa membrane (Sigma-Aldrich). Then ultrafiltrate was then purified on a Bio-Gel P-10 column (2.6 \times 100 cm) eluted with 0.2 M NH4HCO3 to obtain three fractions (SFGG-1, SFGG-2 and SFGG-3).

Total sugar content, fucose (Fuc) content, uronic acid (UA) content, sulfate content, monosaccharide composition and molecular weight were determined as previously described [35]. The molecular weights of the polysaccharides were evaluated by GPC-HPLC on tandem TSKgel Guard SWxl (7 $\mu m,~6.0\times40$ mm), TSKgel G4000 SWxl column (7 $\mu m,~7.8\times300$ mm) and TSKgel G3000 SWxl column (7 $\mu m,~7.8\times300$ mm) with elution in 0.1 M ammonium acetate at a flow rate of 0.6 mL/min at 30 °C with refractive index detection. Seven different molecular weight dextrans (00268-500MG, 00269-100MG, 00270-100MG, 00271-100MG, 00891-100MG, 00892-100MG and 00893-100MG), purchased from Sigma (St.Louis, MO), were used as weight standards.

Electrospray ionization mass spectrometry (ESI-MS) and tandem ESI-MS with collision-induced dissociation (ESI-CID-MS/MS). ESI-MS and MS/MS were performed on a LTQ ORBITRAP XL (Thermo Scientific). The samples were dissolved, centrifuged and analyzed. Mass spectra were registered in the negative ion mode at a flow rate of 5 μ L/min. The capillary voltage was set to -3000 V, and the cone voltage was set at -50 V. The source temperature was 80 $^{\circ}$ C, and the desolvation temperature was 150 $^{\circ}$ C. All spectra were analyzed by Xcalibur.

The samples (30 mg) were deuterium oxide (99.9 %) exchanged twice before dissolving in deuterium oxide (99.9 %). Nuclear magnetic resonance (NMR) spectra were recorded on a Bruker AVANCE III 600 MHz (Billerica, MA) at 25 $^{\circ}$ C or at a Hudson-Bruker SB 800 MHz spectrometer (Bruker BioSpin, Billerica, MA, USA) at 25 $^{\circ}$ C.

2.3. Cell viability assay

The MIN6 pancreatic beta cell line was cultured in high glucose Dulbecco's modified Eagle's medium (DMEM), containing 0.05 % 2-mercaptoethanol (Sigma-Aldrich, Bioreagent, St. Louis, MO, USA), 15 % fetal bovine serum for embryonic stem cells (ES-FBS; Vistech, New Zealand), 100 U/mL penicillin and 100 $\mu\text{g/mL}$ streptomycin (Gibco, Carlsbad, CA, USA) at 37 °C in a humidified atmosphere under 5 % CO $_2$. Hydrogen peroxide (H $_2$ O $_2$) was purchased from Sigma-Aldrich (Sigma-Aldrich, USA).

MIN6 cells were seeded in 96-well plate at a density of 1×10^4 cells per well and pretreated with 125 $\mu mol/L~H_2O_2$ for 2 h at 37 $^{\circ}C$ in a CO_2 incubator. The medium was then replaced with fresh medium containing SFGG at different concentrations (0, 25, 50, 100, and 200 $\mu g/mL)$ and the cells were incubated for 24 h at 37 $^{\circ}C$ in a CO_2 incubator.

Cell viability was measured using cell counting kit-8 (CCK-8) assay (Yeasen Biotech, Shanghai, China) according to the manufacturer's instructions. After experimental treatment, the culture supernatant was removed, and cells were incubated in culture medium containing 10 μL CCK-8 for 1.5 h at 37 °C in the dark. The absorbance in each well was measured at 450 nm using a Multiskan GO microplate reader (Thermo Fisher Scientific, Waltham, MA, USA). Cell viability was calculated as follows: Cell viability (%) = $(A_1-A_0) \, / \, (A_c-A_0) \times 100$, where A_0 is the absorbance of the blank, A_1 is the absorbance of the test group, and A_c is the absorbance of the control.

Table 1Primer sequence.

Gene	Primer (forward)	Primer (reverse)
Actin	GTGACGTTGACATCCGTAAAGA	GCCGGACTCATCGTACTCC
Tnf - α	GAGCACAGAAAGCATGATCCG	GCCACAAGCAGGAATGAGAAG
Nf-κb	CTCTGAACAAAATGCCCCACG	ACGATGCAATGGACTGTCAGG
Cxcl10	TGCCGTCATTTTCTGCCTC	TATGGCCCTCATTCTCACTGG
Cxcr4	TATTGTCCACGCCACCAACAG	CGTCGGCAAAGATGAAGTCAG
Neurod1	GACCCAGAAACTGTCTAAAATAGAGACA	AAGGAGACCAGATCAGGGCTTT
Nkx6.1	CTTCTGGCCCGGAGTGATG	GGGTCTGGTGTTTTCTCTTC
Mafa	CTTCAGCAAGGAGGAGGTCATC	GCGTAGCCGCGGTTCTT
Glut2	TCATCATTGCTGGACGAAGTG	TTGCCCAGAATAAAGCTGAGG
Pdx1	TAGGCGTCGCACAAGAAGAA	TCCGTATTGGAACGCTCAAGT

2.4. Cell cycle assay

MIN6 cells were seeded in 6-well plate at a density of 4×10^5 per well. The cell cycle and apoptosis were then analyzed using commercially available kits (Beyotime, Shanghai, China) according to the manufacturer's instructions. Briefly, after rinsing with phosphate-buffered saline (PBS) and tryptic digestion, the cells were fixed with 75 % ethanol at 4 °C overnight. After discarding the ethanol, the cell pellet was washed with PBS and resuspended in 1 ml of PI staining reagent for 30 min before flow cytometric analysis (BD LSRFortessa, BD Biosciences, San Jose, CA, USA). The percentage of cells in the different phases of the cell cycle was estimated with ModFit LT 5.0 analysis software.

2.5. Senescence-associated β -galactosidase (SA β -gal) assay

The senescence was assessed of MIN6 cells and frozen pancreas sections by X-Gal staining for detection of β -galactosidase activity using commercially available kit (CST, Danvers, MA, USA) after incubation in the fixative solution provided in the kit. The images were taken by optical microscopy (SC180, Olympus, Tokyo, Japan).

2.6. Glucose-stimulated insulin secretion assay (GSIS)

MIN6 cells were preincubated with glucose-free Krebs-Ringer bicarbonate buffer plus HEPES (KRBH) for 30 min before incubation for 1 h in KRBH buffer containing 2.8 mmol/L or 25 mmol/L glucose. The supernatant was collected, and the insulin content was measured by ELISA (Ezassay, Shenzhen, China). The results were normalized by protein concentration.

2.7. Immunofluorescence assay

Pancreas tissues were collected and fixed in 4 % paraformaldehyde (PFA) and dewatered in different concentration of ethanol and embedded in paraffin. After paraffin removal and dehydration in ethanol, the pancreas sections were repaired antigen and incubated with 5 % BSA for 15 min at RT sequentially. MIN6 cells were fixed in 4 % PFA for 20 min, permeabilized with 0.2 % Triton X-100/PBS for 15 min and blocked with 5 % BSA for 60 min at RT. Pancreas sections and cells on coverslips were then incubated overnight at 4 °C with antibodies for the detection of the following: Ki67 (Abcam, Cambridge, UK; dilution 1:300), IL-1β (Abcam: 1:100), γH2AX (Abcam; 1:500), Insulin (Abclonal, Wuhan, China; 1:500), Insulin (Proteintech, USA; dilution 1:1000), FoxO1 (CST, Danvers, MA, USA; 1:200), Glucaogan (Proteintech, USA; dilution 1:800); PDX1(CST, Danvers, MA, USA; 1:400); MAFA (Abcam, 1:250). After several washes with PBS, the fixed cells were incubated for 1.5 h with a goat anti-rabbit and anti-mouse secondary antibody (Invitrogen, Carlsbad, CA, USA; 1:200) and counterstained for 5 min with 4',6-diamidino-2-phenylindole (DAPI) (Sigma-Aldrich, BioReagent; 1:4000) for 5 min. After mounting with fluorescence decay resistant medium, Tissues and cells were observed and photographed under a

confocal microscope (IX83-FV3000, Olympus, Tokyo, Japan) or a fluorescence microscope (Axio Imager M2, ZEISS, Oberkochen, Germany).

2.8. RNA isolation and quantitative real-time PCR (qPCR)

RNA was isolated using AG RNAex Pro reagent (Accurate Biotechnology, Hunan, China) and reversed transcribed using an Evo M-MLV RT Premix kit (Accurate Biotechnology, Hunan, China) according to the manufacturers' protocols. Real-time PCR was performed using the LightCycler480 II system (Roche, Basel, Switzerland) and a SYBR Green Premix Pro Taq Hs qPCR kit (Accurate Biotechnology). After normalization to β -actin, relative gene expression was determined using the $2-\Delta\Delta$ CT method. Primer sequences are as shown in Table 1.

2.9. Western blot assay

MIN6 cells were lysed with cell lysis buffer containing a protease inhibitors cocktail (FdBio Science, Hangzhou, China) and protein concentrations were determined by BCA protein assay kit (FdBio Science). Total protein extracts were denatured and separated by 10 % or 12.5 % sodium dodecyl sulfate-polyacrylamide gel electrophoresis (Millipore, Billerica, MO, USA). Membranes were incubated with primary antibodies for the detection of p16^{Ink4a} (1:1000), p21 (1:1000), p-RB (1:1000), RB (1:1000), EZH2 (1:1000), FoxO1 (1:1000), PDX1 (1:1000), γH2AX (1:1000), Hsp90 (1:5000) (Abcam); p-FoxO1 (1:1000), AKT (1:1000), and p-AKT (1:1000) (CST); E2F1, PI3K (1:1000), p-PI3K (1:1000), and GAPDH (1:10000) (Abclonal); p53 (1:1000) (Proteintech); and β -actin (1:10000) (Sigma) at 4 °C overnight. Subsequently, membranes were incubated with a horseradish peroxidaseconjugated anti-rabbit or anti-mouse secondary antibody (Jackson ImmunoResearch, USA). Proteins were visualized using an enhanced chemiluminescence kit (FdBio Science, Hangzhou, China).

2.10. Animals feeding and grouping

The male C57BL/6 mice, 5 weeks of age, were conducted at Animal Research Center with approval of Animal Ethical and Welfare Committee of Zhejiang Chinese Medical University (ZCMU) (IACUC-20190422-04). The mice were randomly divided into the control group (normal diet) and HFD group (high fat diet: 60 % kcal% fat, D12492, R&D). After 1 month feeding, the HFD group was induced by intraperitoneal injection of 30 mg/kg Streptozotocin (STZ) (freshly dissolved in 0.1 mol/1 sodium citrate buffer pH 4.5) for one day and the control group received the same volume normal buffer. The mice with fasting blood glucose levels \geq 11.1 mmol/L twice was considered as model mice. For metformin (Met) and SFGG treatment, the model mice were divided into three groups:1) the model group were treated with normal water; 2) The metformin group treated with metformin (100 mg/kg); 3) The SFGG group treated with SFGG (100 mg/kg). After 15 weeks intragastrical (i. g.) administration, the mice were euthanized, the tissues were collected.

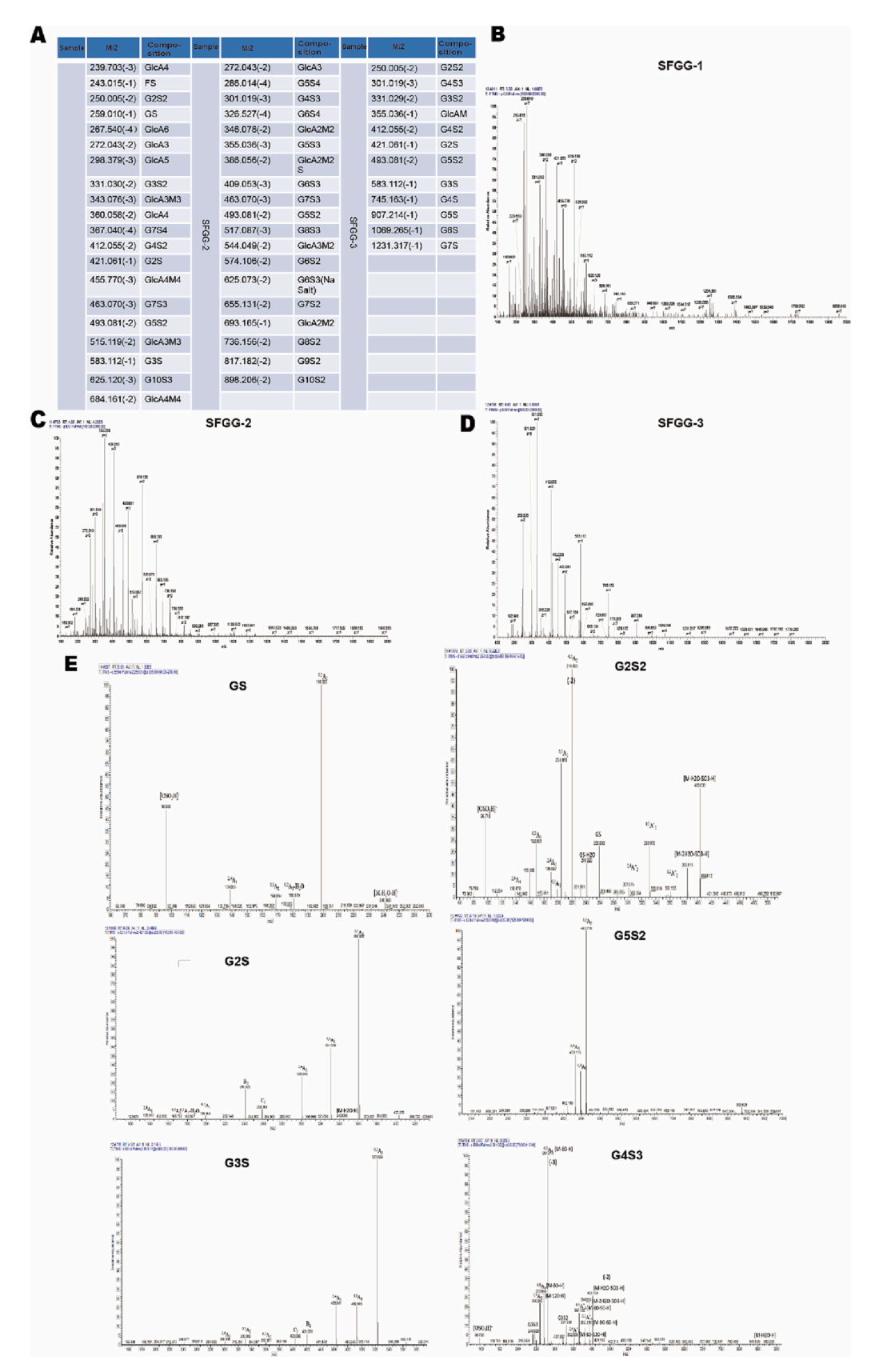


Fig. 2. The structure analysis of SFGG. (A) The primary compositions of SFGG-1, SFGG-2 and SFGG-3, which were summarized in Table. (B-D) Negative-ion mode ESI-MS spectra of SFGG-1, SFGG-2 and SFGG-3. (E) Negative-ion mode electrospray mass spectrometry in tandem with collision-induced dissociation tandem mass spectrometry (ESI-CID-MS/MS) spectra of the compositions.

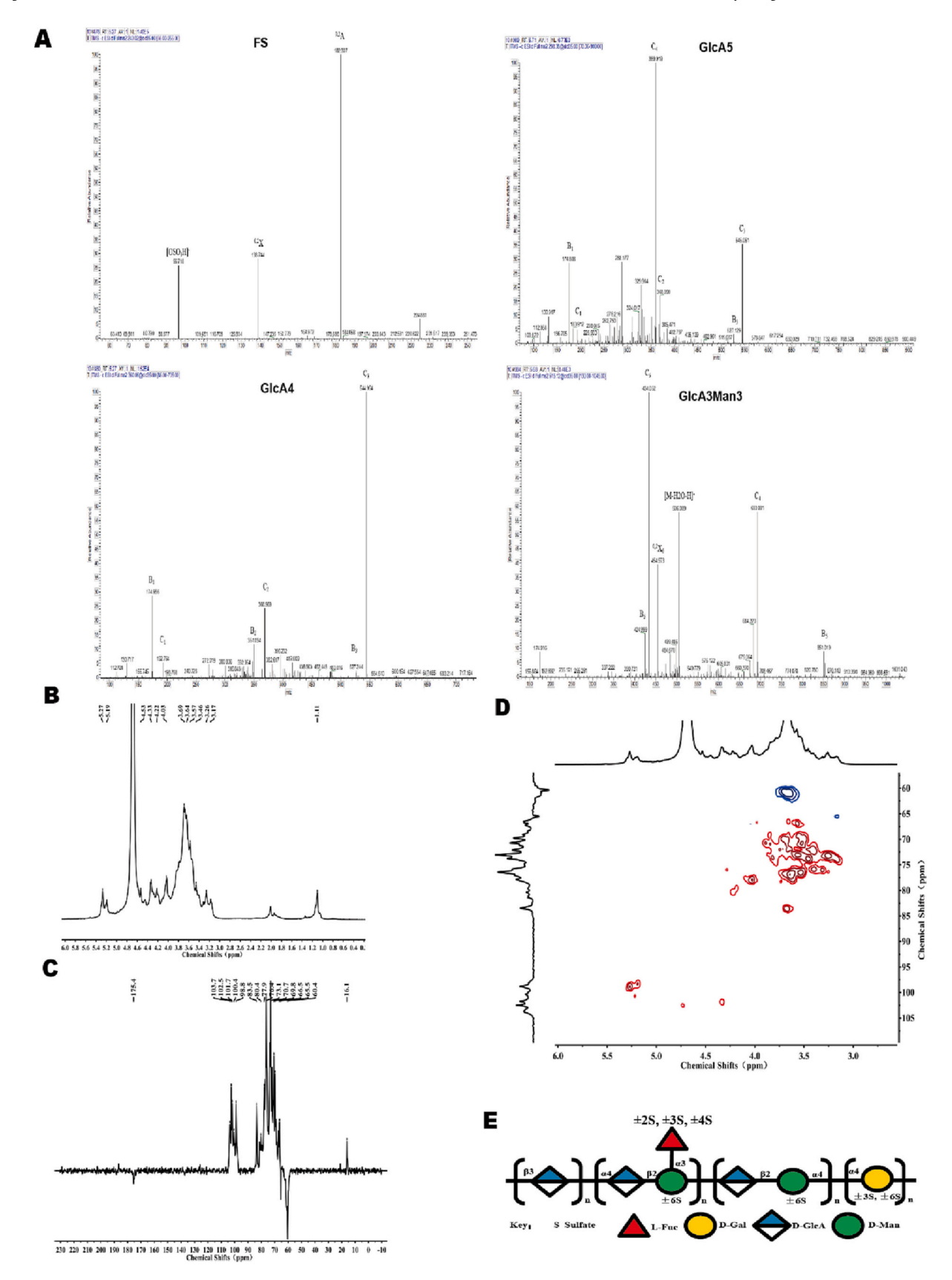


Fig. 3. The structure analysis and features of SFGG. (A) Negative-ion mode electrospray mass spectrometry in tandem with collision-induced dissociation tandem mass spectrometry (ESI-CID-MS/MS) spectra of the compositions. (B) ¹H NMR spectrum of SFGG. (C) DEPTQ spectrum of SFGG. (D) HSQC spectrum of SFGG. (E) Proposed structure of SFGG. Abbreviation: glucuronic acid (GlcA), fucose (F), sulfate (S), galactose (G), mannose (M), number was the degree of polymerization (DP) or the number of sulfate group. For example, GlcA3 stands for glucuronan-trimer. G2S2 stands for di-sulfated galactan-dimer.

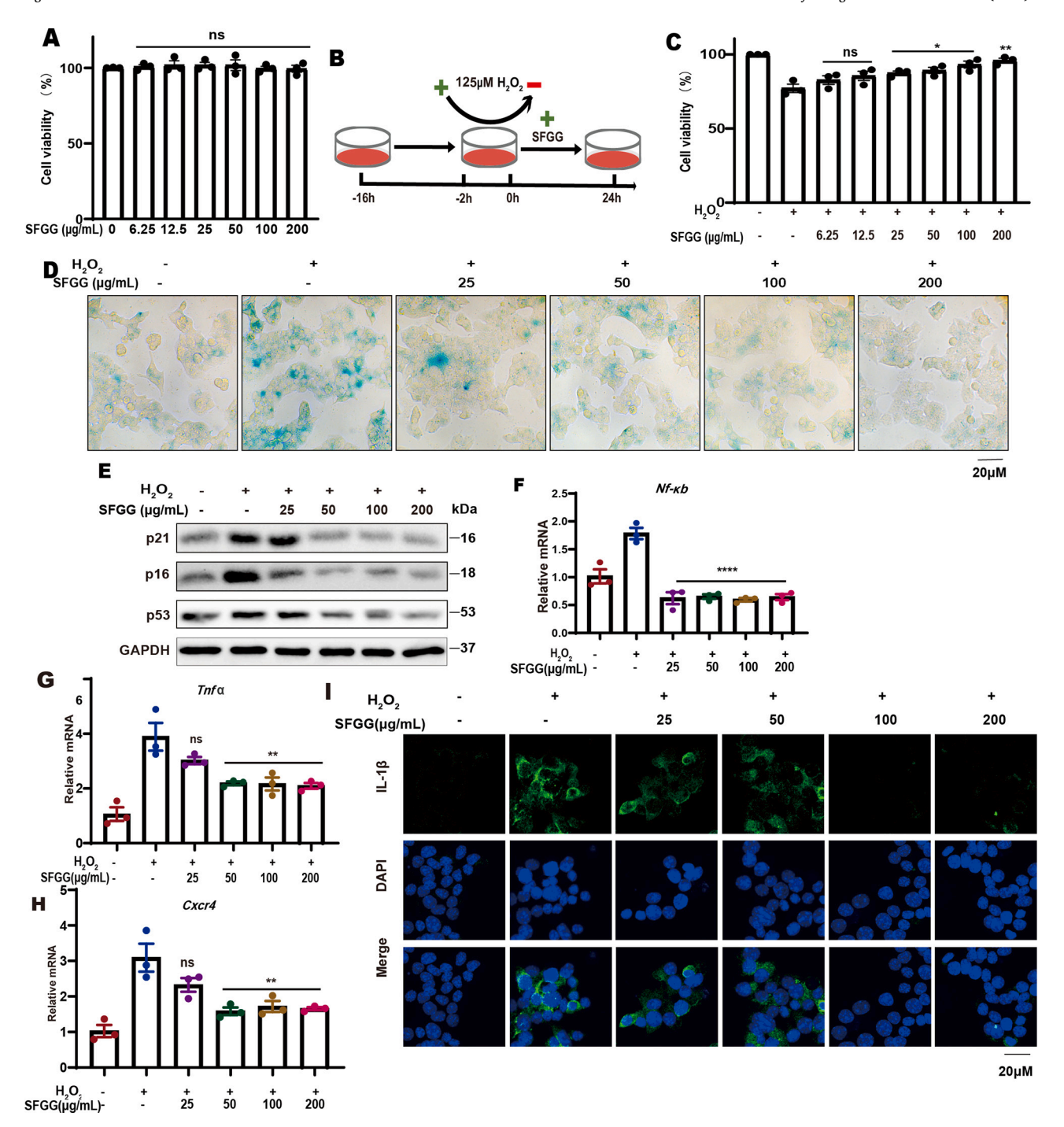


Fig. 4. SFGG alleviated H_2O_2 -induced senescence and SASP factors in MIN6 cells. (A) Cell viability of MIN6 cells after treatment with SFGG in the absence of H_2O_2 exposure (n = 3). (B) Schematic diagram of MIN6 model. (C) Cell viability (n = 3). (D) SA β-gal staining (n = 3). (E) Western blot of p16 INK16a , p21 and p53 (n = 3). (F-H) Quantitative PCR analysis of Nf- κb , Tnf- α and Cxcr4 (n = 3). (I) Immunofluorescence staining of IL-1 β (n = 3). *p < 0.05, **p < 0.01, ****p < 0.0001 vs H_2O_2 control.

2.11. Oral glucose tolerance test (OGTT)

The mice were transferred to fresh cage and fast $14\,h$ before testing $(14\,h)$, while ensuring the drinking water. The blood samples were collected from the tail-vein at 0, 15, 30, 60, 120 min after 1 g/kg body weight of oral glucose administration [36]. The glucose levels were determined using Verio Flex (Johnson, USA). The area under the curve (AUC) was determined from time 0–120 min after glucose administration.

2.12. Hematoxylin and eosin (HE) staining

After paraffin removal and dehydration in ethanol, the pancreas sections were placed in 3 % hydrogen peroxide and incubated with 5 % BSA for 15 min at RT sequentially. Then the sections were treated with DAB kit (CWBIO, China) and taken images using optical microscopy (SC180, Olympus, Tokyo, Japan).

2.13. Statistical analysis

The results are expressed as the mean \pm SEM. One-way ANOVA analysis was used for data comparisons within multiple groups, statistical significance was set at p < 0.05. Prism software was used for graphs and statistical analysis.

3. Results

3.1. Structural analysis of SFGG

Chemical composition analysis indicated that SFGG had a total sugar content of 85.8 % and contained 8.5 % Fuc, 26.9 % UA and 8.9 % sulfate. The PMP derivatization-high performance liquid chromatography (HPLC) spectrum showed that the molar ratio of monosaccharides of SFGG was 1.28:1.38:2.86:1 [mannose (Man): glucuronic acid (GlcA): galactose (Gal): fucose (Fuc)] (Fig. S1A). According to gel permeation chromatography (GPC)-HPLC analysis, the average molecular weight (Mw) of SFGG was approximately 36.1 kDa (Fig. S1B). So, we proposed that SFGG is a sulfated fuco-manno-glucuronogalactan according to the previous study [33].

Polysaccharides with uronic acid are more stable than polysaccharides without uronic acid. So, SFGG was degraded by 0.1 M sulfuric acid and ultrafiltrated by 3 kDa cut-off membrane to study the structural features of galactopyranose residues or fucopyranose residues. The ultrafiltrate was purified on a Bio-Gel P-10 column to obtain three fractions (SFGG-1, SFGG-2 and SFGG-3). The fractions were analyzed by electrospray mass spectrometry mass spectrometry (ESI-MS). SFGG-1 is a mixture of oligo-glucuronan, oligo-glucuronomannan and oligo-sulfated galactan, SFGG-2 contained similar compositions with lower degree of polymerization or sulfation, and SFGG-3 is mainly sulfated oligo-galactan (Fig. 2A-D). Some sulfated oligo-galactans were further analyzed by tandem ESI-MS with collision-induced dissociation (ESI-CID-MS/MS) (Fig. 2E). There were three major characteristic ions ^{0,2}A, ^{0,3}A and ^{2,4}A among sulfated oligo-galactan, suggesting that the linkage of galactan is 1, 4-linked. There were many ions, which were derived from the loss of sulfur trioxide (-80 Da), sulfur trioxide with H_2O (-98 Da) and sulfur trioxide with double H_2O (-116 Da). It was proposed that the sulfate group was substituted at C3 or C6 of galactopyranose residues [37]. Unfortunately, the structural features of oligo-fucans were not detected because the fucopyranose residues might be destroyed or it is branched with sulfated fucose (Monosulfated fucose (FS) was detected). ESI-CID-MS/MS (Fig. 2E) shows that the sulfation pattern of FS might be C2 or C4 because of the presences of $^{0,2}A$ and $^{0,2}X$. In addition, ESI-CID-MS/MS of glucuronan-tetramer and pentamer (Fig. 2E) were performed. There were no characteristic ions ^{0,2}A, indicating that the linkage of glucuronan was 1, 3-linkage. Moreover, in the ESI-CID-MS/MS spectrum of oligo-glucuronomannan (Fig. 2E), there was one characteristic ion ${}^{0,2}A_6$, confirmed the presence of 1, 2-linked α-D-Manp residue. Therefore, we concluded that SFGG had glucuronomannan, glucuronan and sulfated galactan with a backbone of 1, 4linked Galp residues sulfated at C3 or C6. In addition, SFGG might have branches with sulfate fucose.

The 1 H NMR, DEPTQ, HSQC spectra and other two-dimensional spectra of SFGG were also performed (Fig. 3A-D and Fig. S2–4). It is apparent to see that there are five correlated signals at the region of anomeric carbon and hydrogen in the HSQC spectrum (Fig. 3D). We found that resonances with chemical shifts of anomeric hydrogen/carbon at 5.27/98.8, 4.73/102.5 and 4.33/101.7 ppm are characteristic peaks of 1, 2-linked α -D-Manp residues, 1, 3-linked β -D-GlcpA residues and 1, 4-linked β -D-GlcpA residues, respectively [33,38,39]. And the other two correlated signals of 5.19/98.8 and 5.22/100.4 ppm were missing after SFGG was degraded by acid. Thus, we proposed that these two signals belonged to Gal residues and Fuc residues. The molar ratio of Gal to Fuc was 2.86:1 and polysaccharides extracted from brown alga contained only α -L-Fucp residues, suggesting that the strong peak at

5.19/98.8 ppm was belonged to Gal residues while the weak peak at 5.22/100.4 ppm was belonged to Fuc residues. Resonances at 16.1 ppm (Fig. 3C) and 1.11 ppm (Fig. 3B) were typical of CH₃ carbons and hydrogen of Fuc residues. The results in HMBC (Fig. S4) showed that the CH₃ hydrogen of Fuc residues at 1.11 ppm had two strong correlated peaks at 81.4 and 66.5 ppm and one weak correlated peak at 72.3 ppm, which were assigned to C4, C5 and C3 of Fuc residues, respectively. The results in ¹H, ¹H-COSY (Fig. S3) showed that the anomeric hydrogen at 5.22 ppm of Fuc residues had two correlated peaks at 3.85 and 4.22 ppm, suggesting that Fuc residues were sulfated at C2/C3/C4. MS did not detect the structural features of oligo-fucan, proposing that Fuc residues might be branched. According to a previous study [33], sulfated fucose might be branched at C3 of Man residues. And the anomeric hydrogen at 5.22 ppm of Fuc residues in HMBC had the correlated peak at 69.3 ppm, which was assigned to C3 of Man residues. So, we propose that the correlated signals of 5.22/100.4 ppm are α -L-Fucp residues sulfated at C2/C3/C4, which branched at C3 of Man residues. Combined with the MS results, the correlated signals of 5.19/98.8 ppm were the characteristic peaks of 1, 4-linked α-D-Galp residues sulfated at C3 and/ or C6 combined with the MS results. Therefore, we conclude that SFGG is a sulfated fuco-galacto-glucuronomannan, which has the backbones of interspersing 1, 3-linked β-D-GlcpA residues, 1, 4-linked α-D-Galp residues, and alternating 1, 2-linked α-D-Manp residues and 1, 4-linked β-D-GlcpA residues, sulfated at C6 of Man residues, C2/C3/C4 of Fuc residues and C3/C6 of Gal residues, and branched at C3 of Man residues. The proposed structure of SFGG is summarized in Fig. 3E.

3.2. SFGG alleviates senescence and downregulates SASP factors in senescent MIN6 cells

The cytotoxicity and anti-senescence activity of SFGG were evaluated in vitro. As shown in Fig. 4A, there were no significant changes in cell viability after treatment with SFGG at different concentrations (6.25–200 $\mu g/mL$), showing that SFGG had no obvious cytotoxic effects on MIN6 cells. The results indicated that SFGG may be a weakly toxic screening drugs for diabetes.

The previous study showed that $\rm H_2O_2$ induced beta cell senescence, leading to lose beta cell identity and upregulation of SASP factors [6]. Exposed to $125~\mu mol/L~H_2O_2$ for 2 h, the fresh medium containing SFGG at different concentrations was substituted and incubated for 24 h (Fig. 4B-C). Compared with the untreated control cells, exposure to $\rm H_2O_2$ inhibited the viability of MIN6 cells, while this effect was significantly alleviated by SFGG treatment at concentrations ranging from 25 to 200 $\mu g/mL~(p<0.05)$ (Fig. 4C); therefore, we investigated the effects of SFGG at concentrations in this range in the follow-up experiments.

SA β -gal staining showed SFGG markedly alleviated MIN6 cell senescence (Fig. 4D). And senescence-associated proteins, including p16 INK16a, p21 and p53, were dramatically downregulated in a dose-dependent manner after SFGG treatment (Fig. 4E). Senescent cells express and release a variety of SASP factors which typically exacerbate inflammation and systemic insulin resistance by promoting the loss of pancreatic beta cells [10]. The results in Fig. 4F-I confirmed SFGG could downregulated the SASP factors. The gene expression of Nf-xb was downregulated at the concentration of 25-200 μ g/mL (p < 0.0001) (Fig. 4F), Tnf- α and Cxcr4 were downregulated at concentration of 50-200 μ g/mL (p < 0.01) (Fig. 4G-H), and IL-1 β was downregulated obviously at 100-200 μ g/mL compared with the H₂O₂ treatment group (Fig. 4I),. These observations indicated that SFGG could ameliorated beta cell senescence and the accumulation of SASP factors.

3.3. SFGG relieved the suppression of senescent MIN6 cell proliferation and DNA damage

The main feature of cellular senescence is growth inhibition and G1 cell cycle arrest. Ki67 was a key cell proliferation marker to confirm the suppression of MIN6 cell proliferation induced by H_2O_2 treatment, and

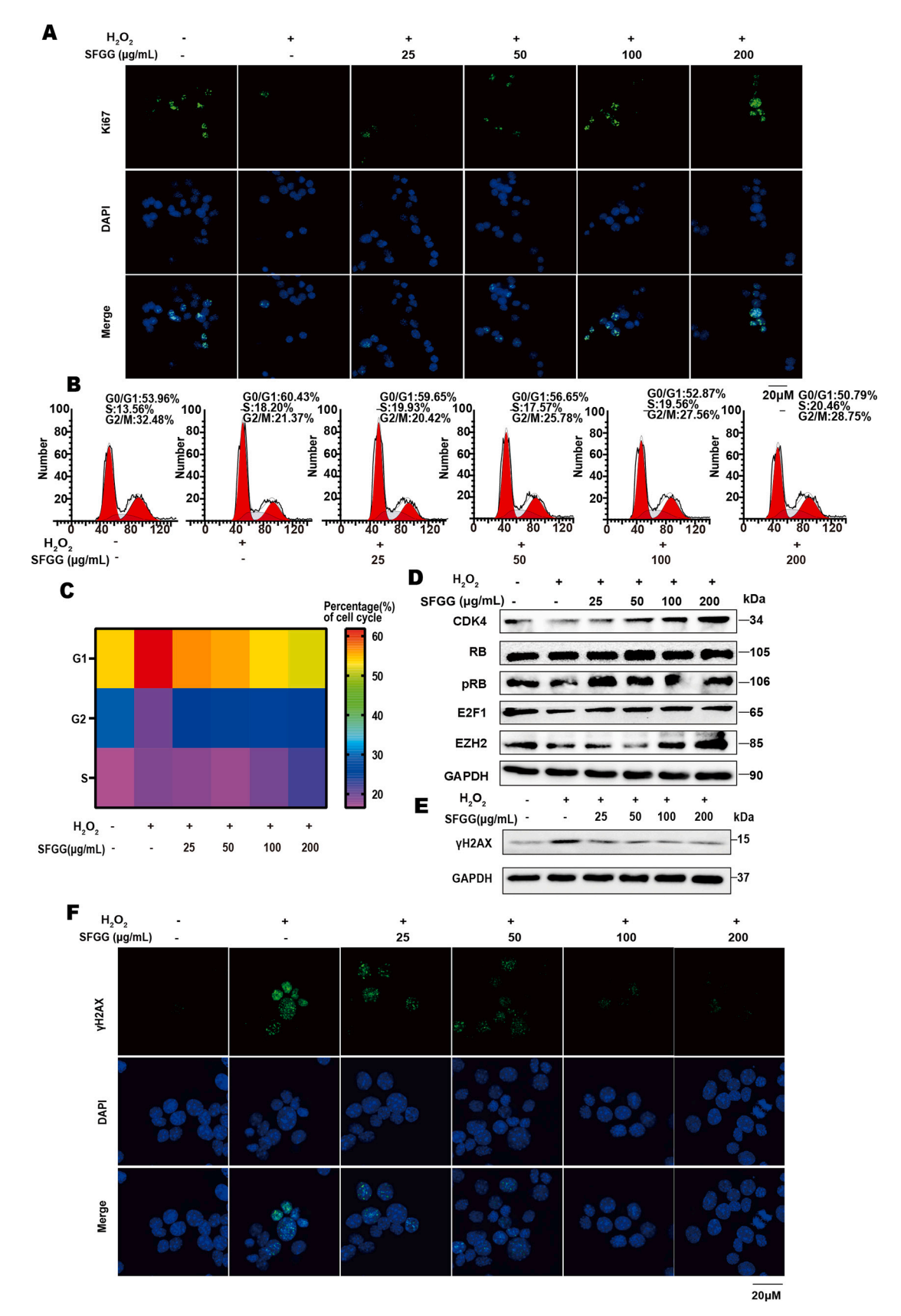


Fig. 5. SFGG alleviated the suppression of senescent MIN6 cell proliferation and relieved the DNA damage. (A) Immunofluorescence staining of Ki67 (n = 3). (B) The Flow cytometric analysis (n = 3). (C) The proportion of cells in each phase of the cycle (n = 3). (D) Western blot of cell cycle regulator proteins(n = 3). (E) Western blot of γ H2AX (n = 3). (F) Immunofluorescence staining of γ H2AX (n = 3).

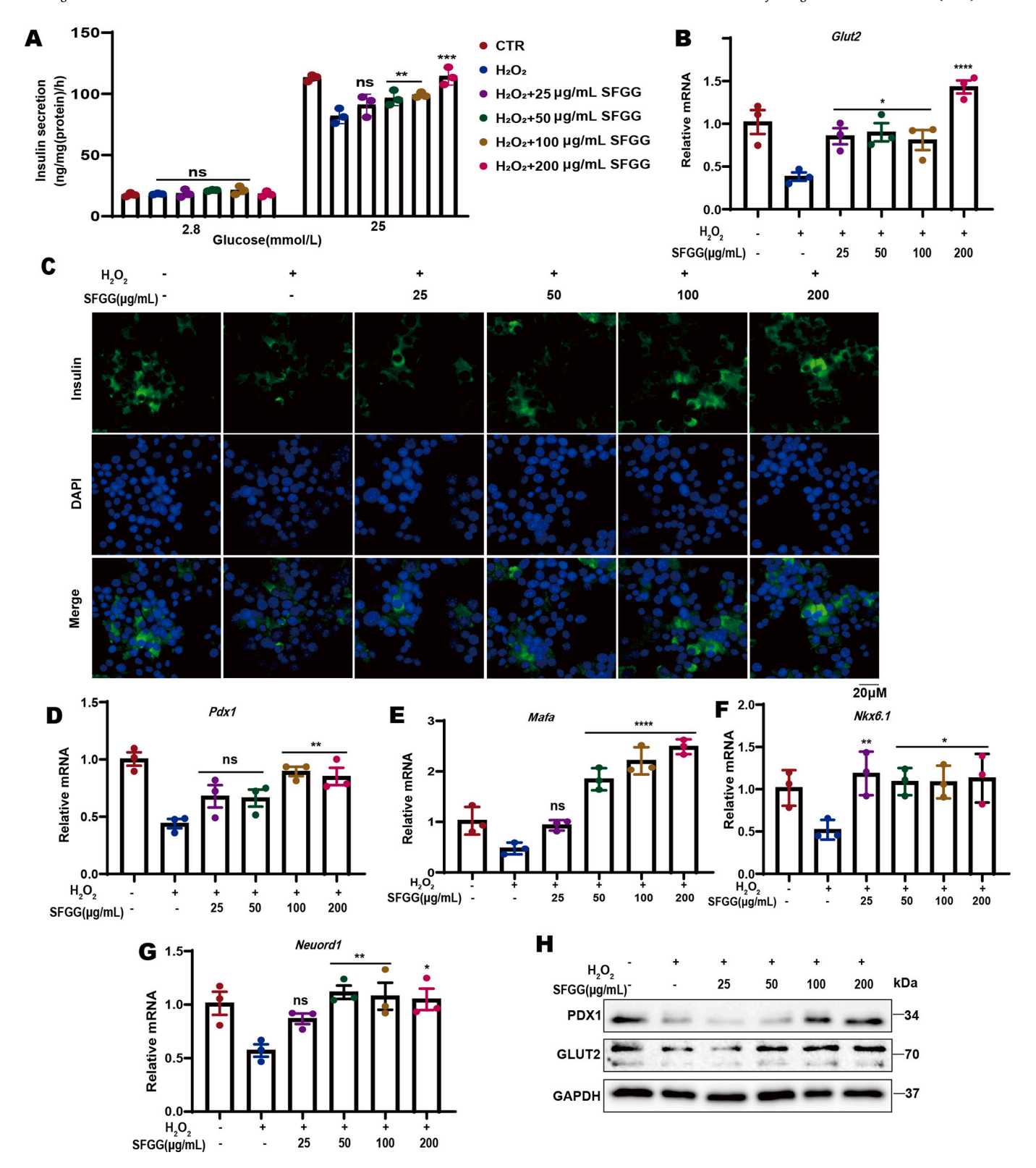


Fig. 6. SFGG modulates insulin synthesis, potentiates glucose-stimulated insulin secretion and beta cell identity. (A) GSIS (n = 3). (B) Gene expression of *Glut2* (n = 3). (C) Immunofluorescence staining of insulin (n = 3). (D-G) Gene expression of (D) Pdx1, (E) Mafa, (F) Nkx6.1, and (G) Neurod1 (n = 3). (H) Western blot of Pdx1 and Glut2 (n = 3). *p < 0.05, **p < 0.01, ****p < 0.001 vs H_2O_2 control.

this effect was eliminated by SFGG administration (Fig. 5A). Furthermore, Flow cytometry showed $\rm H_2O_2$ -treated MIN6 cells were predominantly (60.7 %) distributed in the G0/G1 phase, while a more minor proportion (21.5 %) were distributed in the S phase. Similarly, among the control cells, 56.83 % were distributed in the G0/G1 and 19.06 % in

the S phase (Fig. 5B and C). In contrast, SFGG treatment decreased the proportion of cells in the G1 phase (p < 0.05), while the distribution of cells in the S phase was increased, indicating that SFGG alleviated G1 arrest and promoted the re-entry of cells into the S and G2/M phases. Next, the protein expression of cell cycle regulators, such as CDK4, pRB,

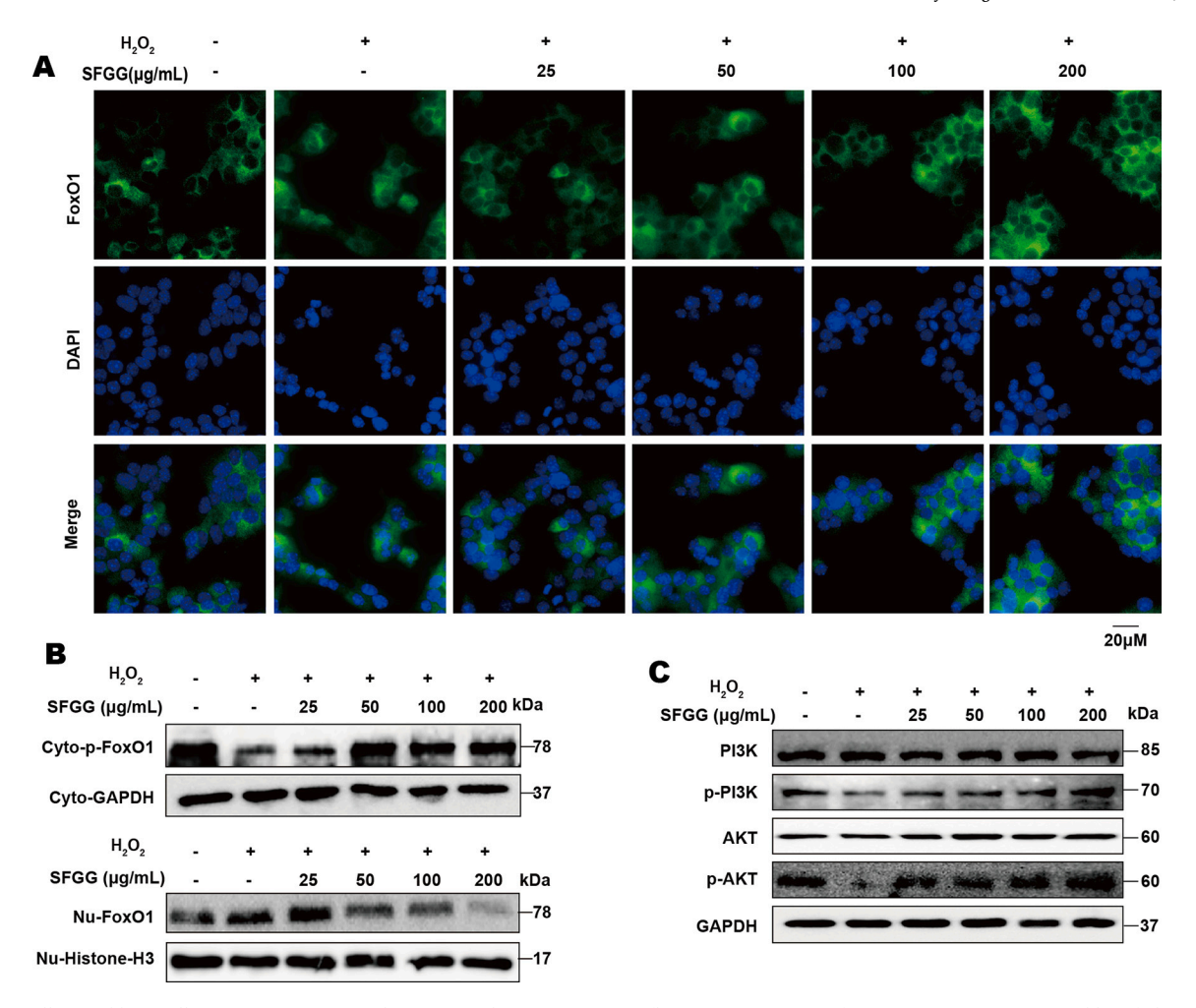


Fig. 7. SFGG alleviated beta cell senescence via PI3K/Akt/Foxo1 pathway. (A) Immunofluorescence staining of FoxO1 (n = 3). (B) Western blot of phosphorylation FoxO1 (p-FoxO1) and FoxO1 in the cytoplasm (Cyto) and nucleus (Nu) (n = 3). (C) Western blot of PI3K/Akt related proteins (n = 3).

E2F1 and EZH2 was upregulated by SFGG treatment (Fig. 5D).

DNA damage accumulation has been recognized as a causal factor in the aging process and the development of age-related pathologies. Following the occurrence of DNA damage, a series of responses are activated in cells that lead to phosphorylation of histone H2AX (γ H2AX), which promotes efficient assembly of DNA repair complexes. Therefore, we performed immunofluorescence and western blot analysis of the expression of γ H2AX, a phosphorylated histone marking double-stranded DNA breaks, to quantify DNA damage in MIN6 cells. The results of immunofluorescence and western blot in Fig. 5E-F showed that SFGG treatment could rescued the accumulation of γ H2AX after H₂O₂ exposure. In other words, SFGG could decreased the DNA damage to alleviate beta cell senescence.

3.4. SFGG modulates insulin synthesis and potentiates GSIS in senescent MIN6 cells

Pancreatic beta cells secrete insulin via a process that is activated by the entry of glucose mediated by glucose transporters to maintain glucose homeostasis. After exposure to $\rm H_2O_2$, insulin secretion at 25 mmol/L glucose was decreased compared with untreated control cells and the function was enhanced by SFGG treatment at 50, 100 and 200 $\rm \mu g/mL$ (p < 0.05). However, there was no difference at low-glucose stimulation (Fig. 6A). Furthermore, Glut2, controlling the entry of glucose into cells, were upregulated by SFGG treatment in a dose-dependent manner (p < 0.05) (Fig. 6B and H).

Moreover, the insulin synthesis was significantly suppression after

H₂O₂ treatment (Fig. 6C). Insulin synthesis in response to glucose and insulin signaling is controlled largely by binding of key transcription factors (PDX1, MAFA, NKX6.1 and Neurod1) to upstream enhancer elements as well as numerous coregulators [40–42]. The expression of these transcription factors genes was downregulated in MIN6 cells following exposure to H₂O₂ and upregulated by SFGG treatment. The gene and protein expression of Pdx1 were upregulated at the concentration of 100-200 μ g/mL (p < 0.01) (Fig. 6D and H). The gene expression of Mafa was upregulated at concentration of 50-200 μg/mL in a dose-dependent manner (p < 0.0001) (Fig. 6E), Nkx6.1 was upregulated at concentration of 25–200 μ g/mL (25 μ g/mL, p < 0.01; 50–200 $\mu g/mL$, p < 0.05) (Fig. 6F), and Neurod1 was upregulated at concentration of 50–200 µg/mL (50–100 µg/ml, p < 0.01; 200 µg/mL, p < 0.05) compared with the H₂O₂ treatment group (Fig. 6G). All together, The SFGG could modulate insulin synthesis, potentiated insulin secretion and recovered beta cell identity in senescent MIN6 cells.

3.5. SFGG ameliorates senescence by inhibition of the FoxO1 via PI3K/AKT pathway

FoxO1 regulation of cell proliferation, apoptosis, differentiation, and insulin secretion in pancreatic beta cells is mediated by transcription factors such as MAFA and Neurod1 [42,43]. In this study we found that FoxO1 phosphorylation was markedly decreased in MIN6 cells treated with $\rm H_2O_2$ compared with the levels in the control group and that this effect was alleviated by SFGG treatment at cytoplasm, and the FoxO1 expression was conversely at nucleus (Fig. 7B). FoxO1 is known to

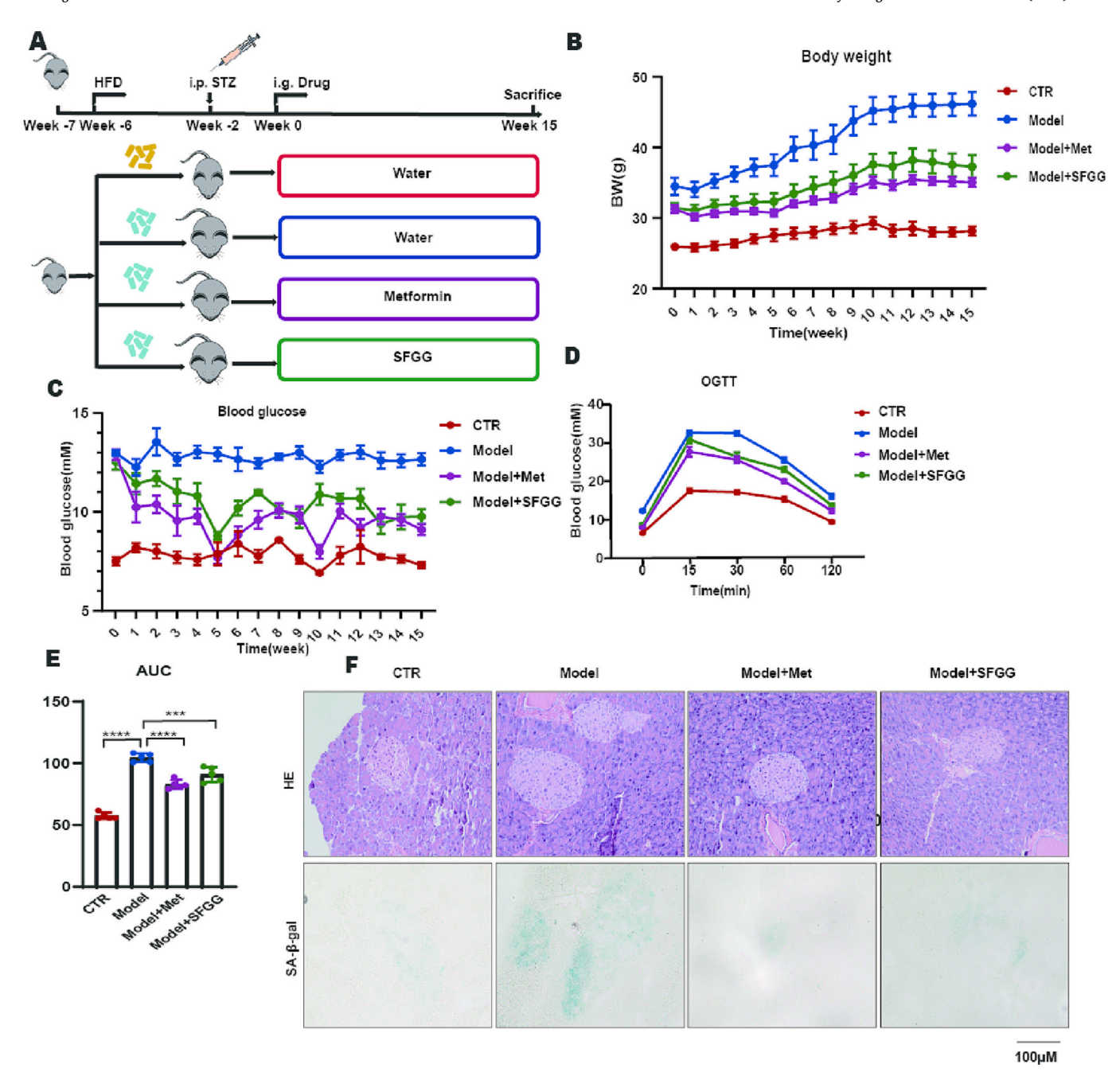


Fig. 8. SFGG ameliorate pancreatic beta cell function in diabetic mice. (A)The flow diagram of mice model. (B) Body weight monitoring (n = 5). (C) Blood glucose monitoring (n = 5). (D-E) OGTT and AUC (n = 5). (F) HE and SA β -gal staining of pancreas (n = 5). ***p < 0.001, ****p < 0.0001 vs model group.

shuttle between nucleus and cytoplasm to regulate various biological activities. Dephosphorylation of FoxO1 results in its translocation to the nucleus from the cytoplasm and inactivation of its transcription factor capability. The results of immunofluorescence staining and western blot showed that FoxO1 was translocated to nucleus in MIN6 cells exposed to $\rm H_2O_2$ and that the translocation was reversed by SFGG treatment (Fig. 7A).

Many studies indicated that the PI3K/AKT signaling pathway involved in regulating the proliferation and function of pancreatic beta cells, and PI3K/AKT pathway could inhibit FoxO1 translocation [44,45]. Therefore, we analyzed the expression of proteins related to the PI3K/AKT pathway, which regulates FoxO1 translocation to further characterize the molecular mechanisms underlying the protective effects of SFGG against senescence. Western blot analysis showed that the phosphorylation of PI3K and AKT was decreased in MIN6 cells exposed to

 $\rm H_2O_2$ compared with the levels in the control group and this effect was completely alleviated by SFGG treatment (Fig. 7C). The results demonstrated that SFGG could ameliorates beta cell senescence by inhibition of the FoxO1 translocation via PI3K/AKT pathway.

3.6. SFGG decelerated pancreatic beta cell senescence in mice

The C57BL/6 mouse model was attended in the following study after 4 weeks HFD and 30 mg/kg STZ injection one time to further the translation potential of studies in vivo (Fig. 8A). Interestingly, mice from SFGG group displayed a significant decrease of body weight (p < 0.0001) and blood glucose (p < 0.0001) compared with the model group and the hypoglycemic capacity was as good as metformin after 15 weeks SFGG administration (Fig. 8B-C). Furthermore, the glucose tolerance was deteriorated at model group, as judged by OGTT. The SFGG can

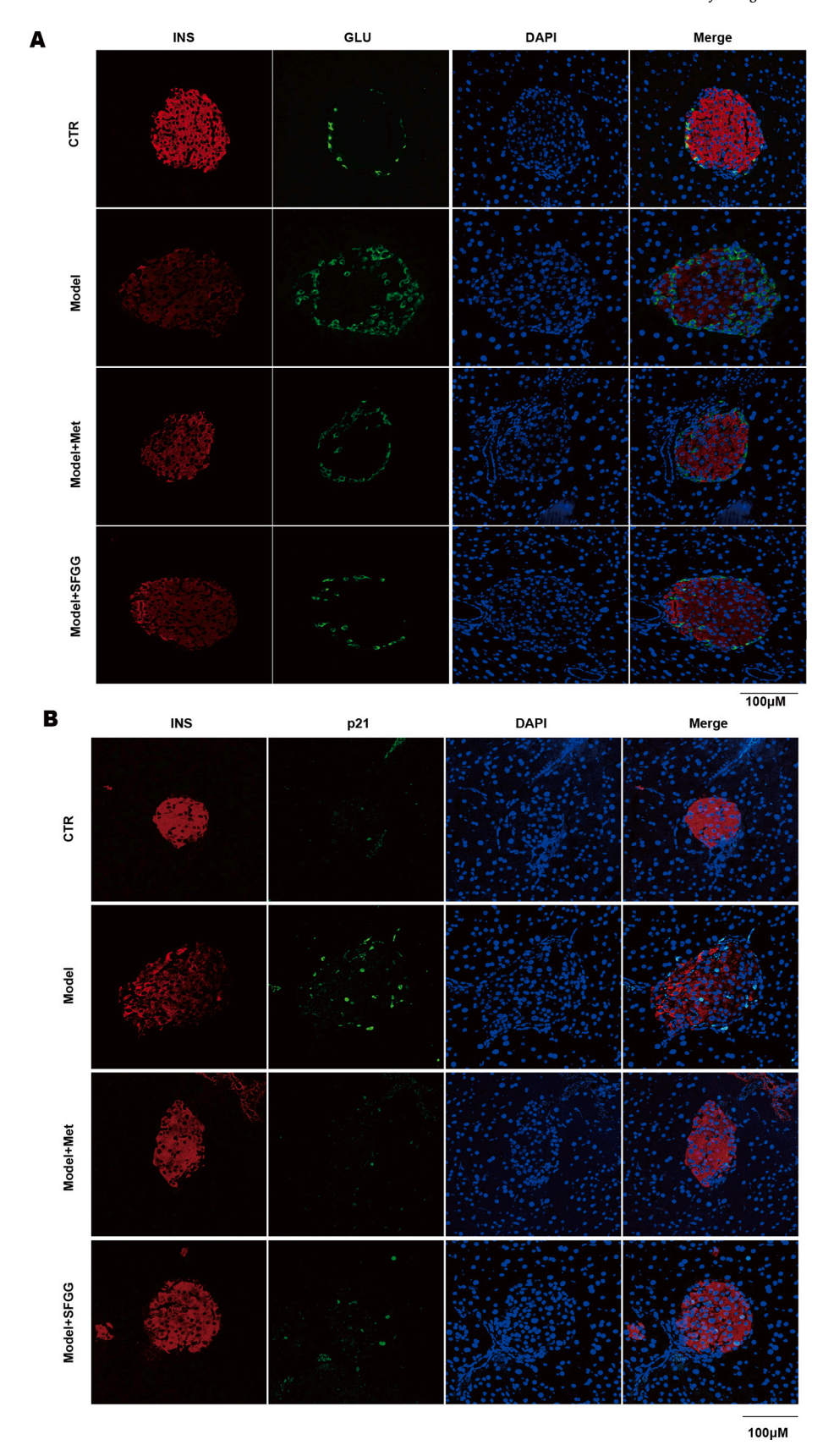


Fig. 9. SFGG alleviate pancreatic beta cell senescence in diabetic mice. (A) Immunofluorescence of insulin (INS) and glucagon (GLU) (n = 5). (B) Immunofluorescence of INS and p21 (n = 5).

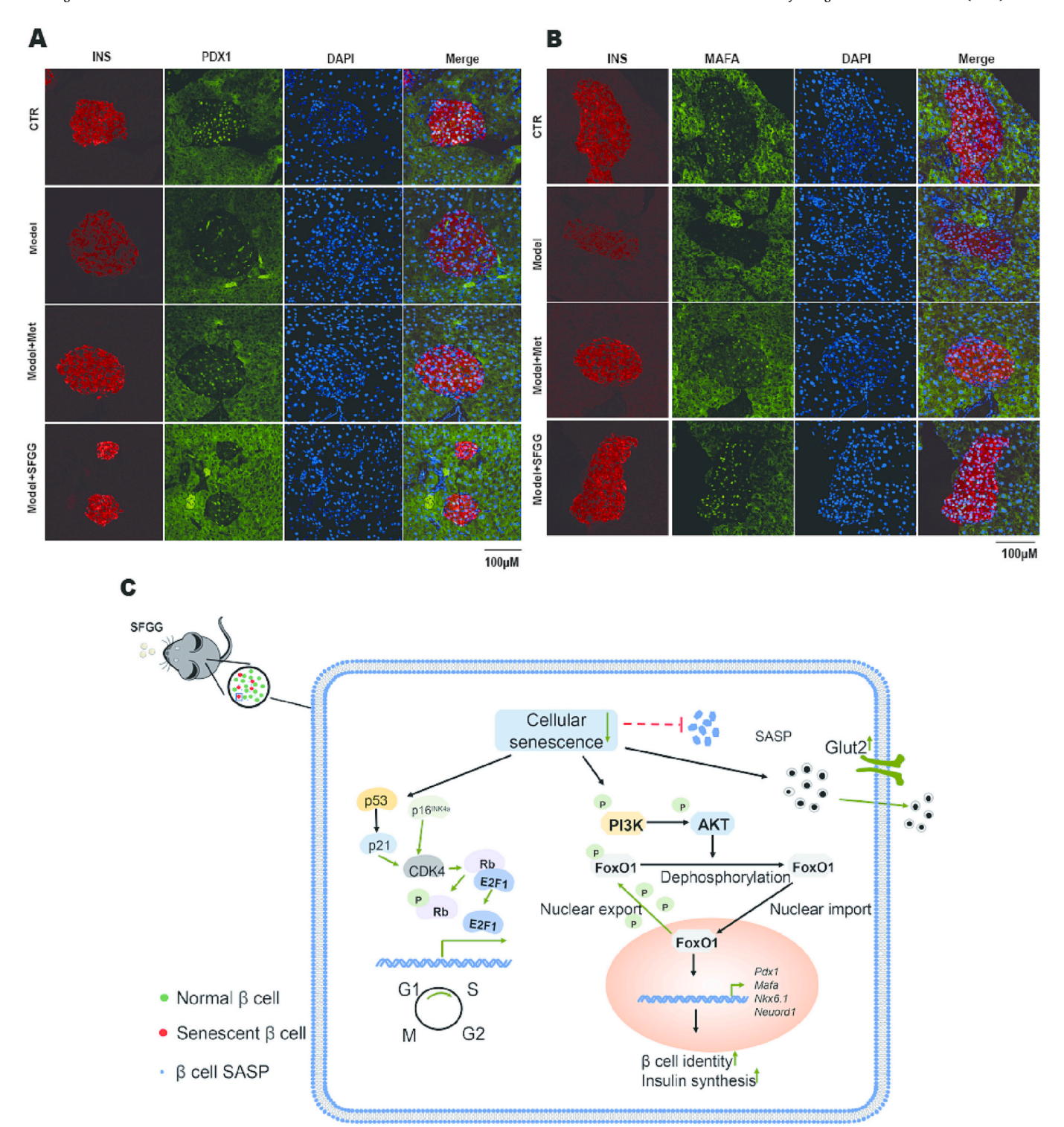


Fig. 10. SFGG improved beta cell identity in mice model. (A) Immunofluorescence of INS and PDX1 (n = 5). (B) Immunofluorescence of INS and MAFA (n = 5). (C) Schematic diagram of the proposed mechanism. SFGG can strengthen beta cell identity and insulin secretion by downregulating the p53/p21 and p16 pathways, restoring the normal cell cycle and inhibiting the SASP factors. SFGG attenuated senescence and improved beta cell function via PI3K/AKTF0xO1 signaling pathway.

improved the glucose tolerance obviously, the AUC was reduced obviously at SFGG group (p < 0.001) (Fig. 8D-E). HE staining showed the beta cell mass was reduced at SFGG group, and the insulin level in islets was improved and glucagon was downregulated at SFGG group (Figs. 8F and 9A). All the results indicated that the SFGG can improved the islets function of the mouse model.

We then examined that SA β -gal staining and p21⁺ins⁺ cells were decreased significantly in islets of SFGG mice compared to model group,

suggesting that the SFGG could inhibit beta cell senescence (Figs. 8F and 9B). The previous study showed the SFGG can enhance expression of key beta cell identity genes, including *a, Pdx1, Nkx6.1* and *Neurod1* in MIN6 cell. We further detected the expression of PDX1 and MAFA in islets, The results showed that the key beta cell identity markers are significantly upregulated in SFGG group compared with model group (Fig. 10A-B). These findings suggest that the SFGG inhibits beta cell senescence and improved beta cell identity.

Above all, we know that SFGG can downregulate the p53/p21 and p16 pathways to enhance cell cycle regulators such as CDK4, pRB, E2F1 and EZH2 and restore the normal cell cycle. SFGG can also inhibit the SASP factors to reduce inflammatory damage to cell function. Moreover, SFGG can strengthen beta cell identity and insulin synthesis via the PI3K/AKT/FOXO1 pathway. All these changes will enhance cellular activity and insulin secretion in pancreatic beta cells (Fig. 10C). The results suggested SFGG are a potential drug for beta cell senescence and alleviation of the progression of T2D.

4. Discussion

Fucoidan has numerous biological activities, such as anti-inflammatory, anti-senescence, anti-tumor, antioxidant, anti-hyperlipidemia and so on [5–8]. However, the structures of fucoidan are very complex. In this study, a sulfated fuco-manno-glucuronogalactan (SFGG) was prepared. Structural analysis indicated that it has the backbones of interspersing 1, 3-linked β -D-GlcpA residues, 1, 4-linked α -D-GlcpA residues, and alternating 1, 2-linked α -D-Manp residues and 1, 4-linked β -D-GlcpA residues, sulfated at C6 of Man residues, C2/C3/C4 of Fuc residues and C3/C6 of Gal residues, and branched at C3 of Man residues. Owing to targeting pancreas beta cell senescence is a potential therapeutic strategy for T2D therapies, we hypothesised SFGG was a potential drug to ameliorate senescent pancreatic beta cells.

The senescence phenotype is often characterized by increased β-galactosidase activity and DNA damage as well as cell cycle arrest and enhanced secretion of SASP factors [46]. SFGG treatment can obviously alleviated DNA damage and SA-β-gal activity, indicating its potential as an anti-senescence drug. Moreover, cell cycle arrest, which is regulated by multiple proteins, such as p16^{INK4a} and p21. p16 inhibits CDK4/6 directly and is regarded as a unique and specific marker of senescence. p21 inhibits a series of CDKs and its expression is regulated mainly by p53. Thus, fucoidan can prevent and treat cell cycle arrest by regulating the expression of p16^{INK4a}, p21 and p53 in MIN6 cells [46]. Furthermore, CDK4 forms a complex with cyclin D to phosphorylate RB, which then triggers the disassociation of RB and E2F to promote cell cycle transition to the S phase [47]. In accordance with these findings, we showed that SFGG treatment rescued the arrest of cell cycle progression from the G0/G1 phase to S phase, and increased the expression of CDK4, phosphorylated RB and E2F1. Senescent cells secrete cytokines, chemokines and proteinases, which are highly heterogeneous and affect a series of biological processes. Our study showed the IL-1 β , NF- κ B, TNF- α and CXCR4 were upregulated in senescent MIN6 cells, and that these effects were alleviated by SFGG treatment, indicating the therapeutic activity of SFGG on senescence in MIN6 cells.

The accumulation of senescent beta cells leads to the loss of functional beta cell mass and ultimately, to deficient insulin secretion, which are key contributors to age-related T2D [10]. Aging rats have defects in the transduction of glucose-induced stimulatory signals that regulate insulin secretion and synthesis [48]. In the present study, we demonstrated that SFGG facilitated insulin synthesis and ameliorated the insufficiency of insulin secretion in senescent MIN6 cells and islets of diabetic mice. Furthermore, insulin synthesis and secretion are regulated mainly by MAFA, NKX6.1, PDX1, Neurod1, which are vital to beta cell function and identity [41,42]. In this study, SFGG could upregulated the expression of PDX1, NKX6.1, MAFA, and Neurod1 in senescent cells. Thus, it was found that SFGG could alleviate senescent beta cell dysfunction and loss of identity.

A series of studies showed that FoxO1 is a negative regulator of the transcription factor PDX1 and highly expressed in pancreatic beta cells, which has a direct effect on pancreatic beta cell neogenesis, proliferation, insulin secretion and stress resistance [43,49–51]. The PI3K/AKT signaling pathway is central to the control of autophagy, metabolism, and oxidative stress [52] and is involved in the regulation of beta cell mass and function [53,54]. It has been reported that phycocyanin, a

pigment protein purified from alga, exerted protective effects against INS-1 pancreatic beta cells dysfunction by modulating the PI3K/AKT signaling pathway [55,56]. FoxO1 activity is regulated by phosphorylation mediated by the PI3K and AKT. Phosphorylation of FoxO1 by AKT leads to its translocation from the nucleus to the cytoplasm, resulting in the inhibition of FoxO1-dependent transcription [57,58]. It was shown that SFGG could affected translocation FoxO1 and activation of PI3K/AKT pathway involving in the mechanism of SFGG reducing senescent beta cells.

5. Conclusion

In summary, we demonstrated that SFGG could effectively alleviated senescence-related phenotypes in vitro and in vivo, suggesting that SFGG is implicated as a potential agent for the treatment of beta cell senescence and alleviation the progression of T2D. Protective effects against senescence of beta cell function via PI3K/AKT/FoxO1 signaling pathway may play a vital role in alleviating pancreatic beta cell senescence.

CRediT authorship contribution statement

Wenjing Zhang: Conceptualization, methodology, data acquisition, investigation, formal analysis, writing-original draft preparation, writing-reviewing and editing, project administration; funding acquisition; Nan Wu: Data acquisition, formal analysis, writing-original draft preparation; Hong Wang: Data acquisition; Genxiang Mao: Writing-reviewing, methodology; Xiaojun Yan: Writing-reviewing and editing; Fuming Zhang: Writing Reviewing, Editing and funding acquisition; Robert J. Linhardt: Writing Reviewing, Editing and funding acquisition; Weihua Jin: Resources, data curation, formal analysis, writing-original draft preparation, supervision, funding acquisition, project administration; Jiaqiang Zhou: Data curation, writing-reviewing, editing, project administration, funding acquisition, and supervision.

Declaration of competing interest

We have no financial interests/personal relationships with other people or organizations that can inappropriately influence our work, and no other conflict of interest exists.

Data availability

Data will be made available on request.

Acknowledgments

This study was supported by the National Natural Science Foundation of China (No. 41906095 to W.Z. and 81870562 and 82270857 to J. Z.), the National Key Technology R&D Program of China (No. 2009BAI80B02 to J.Z.), the Zhejiang Provincial Natural Science Foundation of China (No. LY22D060003 to W.Z., LZ22H070002 to J.Z. and LY19D060006 to W.J.), the GlycoMIP a Science Foundation Materials Innovation Platform (DMR-1933525 to F.Z. and R.J.L.), and the Open Fund of Key Laboratory of Experimental Marine Biology, Chinese Academy of Sciences (No. KF2018NO2 to W.J.).

Appendix A. Supplementary data

Supplementary data to this article can be found online at https://doi.org/10.1016/j.ijbiomac.2023.123846.

References

 P. Saeedi, I. Petersohn, P. Salpea, et al., Global and regional diabetes prevalence estimates for 2019 and projections for 2030 and 2045: results from the

- International Diabetes Federation Diabetes Atlas, 9(th) edition, Diabetes Res. Clin. Pract. 157 (2019), 107843, https://doi.org/10.1016/j.diabres.2019.107843.
- [2] C. Aguayo-Mazzucato, S. Bonner-Weir, Pancreatic β cell regeneration as a possible therapy for diabetes, Cell Metab. 27 (2018) 57–67, https://doi.org/10.1016/j. cmet.2017.08.007.
- [3] L.I. Hudish, J.E. Reusch, L. Sussel, β cell dysfunction during progression of metabolic syndrome to type 2 diabetes, J. Clin. Invest. 129 (2019) 4001–4008, https://doi.org/10.1172/jci129188.
- [4] G.C. Weir, Glucolipotoxicity, β-cells, and diabetes: the emperor has no clothes, Diabetes 69 (2020) 273–278, https://doi.org/10.2337/db19-0138.
- [5] D.G.A. Burton, R.G.A. Faragher, Obesity and type-2 diabetes as inducers of premature cellular senescence and ageing, Biogerontology 19 (2018) 447–459, https://doi.org/10.1007/s10522-018-9763-7.
- [6] C. Aguayo-Mazzucato, J. Andle, T.B. Lee Jr., et al., Acceleration of β cell aging determines diabetes and senolysis improves disease outcomes, Cell Metab. 30 (2019) 129–142.e4, https://doi.org/10.1016/j.cmet.2019.05.006.
- [7] G. Giovos, M.P. Yavropoulou, in: The role of cellular senescence in diabetes mellitus and osteoporosis: molecular pathways and potential interventions 18, 2019, pp. 339–351, https://doi.org/10.1007/s42000-019-00132-6.
- [8] M. Halim, A. Halim, The effects of inflammation, aging and oxidative stress on the pathogenesis of diabetes mellitus (type 2 diabetes), Diabetes Metab. Syndr. 13 (2019) 1165–1172, https://doi.org/10.1016/j.dsx.2019.01.040.
- [9] A.K. Palmer, B. Gustafson, J.L. Kirkland, et al., Cellular senescence: at the nexus between ageing and diabetes, Diabetologia 62 (2019) 1835–1841, https://doi.org/ 10.1007/s00125-019-4934-x.
- [10] N. Li, F. Liu, P. Yang, et al., Aging and stress induced β cell senescence and its implication in diabetes development, Aging (Albany NY) 11 (2019) 9947–9959, https://doi.org/10.18632/aging.102432.
- [11] A. Helman, D. Avrahami, A. Klochendler, et al., Effects of ageing and senescence on pancreatic β-cell function, Diabetes Obes. Metab. 18 (Suppl 1) (2016) 58–62, https://doi.org/10.1111/dom.12719.
- [12] X. Zhu, Z. Chen, W. Shen, et al., Inflammation, epigenetics, and metabolism converge to cell senescence and ageing: the regulation and intervention, Signal Transduct. Target. Ther. 6 (2021) 245, https://doi.org/10.1038/s41392-021-00646.9
- [13] Y. Li, W. Deng, J. Wu, et al., TXNIP exacerbates the senescence and ageing-related dysfunction of β-cells by inducing cell cycle arrest through p38–p16/p21-CDK-rb pathway, Antioxid. Redox Signal. (2022), https://doi.org/10.1089/ars.2021.0224.
- [14] J. Birch, J. Gil, Senescence and the SASP: many therapeutic avenues, Genes Dev. 34 (2020) 1565–1576, https://doi.org/10.1101/gad.343129.120.
- [15] S. Khosla, J.N. Farr, in: The role of cellular senescence in ageing and endocrine disease 16, 2020, pp. 263–275, https://doi.org/10.1038/s41574-020-0335-y.
- [16] H.A. Hirsch, D. Iliopoulos, K. Struhl, Metformin inhibits the inflammatory response associated with cellular transformation and cancer stem cell growth, Proc. Natl. Acad. Sci. U. S. A. 110 (2013) 972–977, https://doi.org/10.1073/ pnas.1221055110.
- [17] Z. Lv, Y. Guo, Metformin and its benefits for various diseases, Front. Endocrinol. 11 (2020) 191, https://doi.org/10.3389/fendo.2020.00191 (Lausanne).
- [18] X. Wang, K. Yi, Y. Zhao, Fucoidan inhibits amyloid-β-induced toxicity in transgenic Caenorhabditis elegans by reducing the accumulation of amyloid-β and decreasing the production of reactive oxygen species, Food Funct. 9 (2018) 552–560, https:// doi.org/10.1039/c7fo00662d.
- [19] L. Zhang, J. Hao, Y. Zheng, et al., Fucoidan protects dopaminergic neurons by enhancing the mitochondrial function in a rotenone-induced rat model of Parkinson's disease, Aging Dis. 9 (2018) 590–604, https://doi.org/10.14336/ ad.2017.0831.
- [20] J.H. Ahn, M.C. Shin, D.W. Kim, et al., Antioxidant properties of fucoidan alleviate acceleration and exacerbation of hippocampal neuronal death following transient global cerebral ischemia in high-fat diet-induced obese gerbils 20, 2019, https:// doi.org/10.3390/ijms20030554
- [21] P.M. Chang, K.L. Li, Y.C. Lin, Fucoidan-fucoxanthin ameliorated cardiac function via IRS1/GRB2/ SOS1, GSK3β/CREB pathways and metabolic pathways in senescent mice, Mar. Drugs 17 (2019), https://doi.org/10.3390/md17010069.
- [22] E. Apostolova, P. Lukova, A. Baldzhieva, et al., Immunomodulatory and antiinflammatory effects of fucoidan: a review, Polymers 12 (2020), https://doi.org/ 10.3390/polym12102338 (Basel).
- [23] S. Song, H. Peng, Q. Wang, et al., in: Inhibitory activities of marine sulfated polysaccharides against SARS-CoV-2 11, 2020, pp. 7415–7420, https://doi.org/ 10.1039/d0fo02017f.
- [24] Q. Wu, S. Wu, Y. Cheng, et al., in: Sargassum fusiforme fucoidan modifies gut microbiota and intestinal metabolites during alleviation of hyperglycemia in type 2 diabetic mice 12, 2021, pp. 3572–3585, https://doi.org/10.1039/d0fo03329d.
- [25] B. Mabate, C.D. Daub, S. Malgas, Fucoidan structure and its impact on glucose metabolism: implications for diabetes and cancertherapy 19, 2021, https://doi. org/10.3390/md19010030.
- [26] Y. Zhang, J. Zuo, L. Yan, et al., in: Sargassum fusiforme fucoidan alleviates high-fat diet-induced obesity and insulin resistance associated with the improvement of hepatic oxidative stress and gut microbiota profile 68, 2020, pp. 10626–10638, https://doi.org/10.1021/acs.jafc.0c02555.
- [27] W.C. Yu, Y.L. Chen, P.A. Hwang, et al., Fucoidan ameliorates pancreatic β-cell death and impaired insulin synthesis in streptozotocin-treated β cells and mice via a Sirt-1-dependent manner, Mol. Nutr. Food Res. 61 (2017), https://doi.org/10.1003/synfr.201700136.
- [28] X. Jiang, J. Yu, Z. Ma, et al., Effects of fucoidan on insulin stimulation and pancreatic protection via the cAMP signaling pathway in vivo and in vitro, Mol. Med. Rep. 12 (2015) 4501–4507, https://doi.org/10.3892/mmr.2015.3989.

- [29] E.Y. Min, I.H. Kim, J. Lee, et al., The effects of fucodian on senescence are controlled by the p16INK4a-pRb and p14Arf-p53 pathways in hepatocellular carcinoma and hepatic cell lines, Int. J. Oncol. 45 (2014) 47–56, https://doi.org/ 10.3892/ijo.2014.2426.
- [30] J.H. Lee, S.H. Lee, S.H. Choi, et al., The sulfated polysaccharide fucoidan rescues senescence of endothelial colony-forming cells for ischemic repair, Stem Cells 33 (2015) 1939–1951. https://doi.org/10.1002/stem.1973.
- [31] J.H. Lee, C.W. Yun, J. Hur, et al., Fucoidan rescues p-cresol-induced cellular senescence in mesenchymal stem cells via FAK-Akt-TWIST Axis 16, 2018, https://doi.org/10.3390/md16040121.
- [32] Y. Zhang, M. Xu, C. Hu, et al., Sargassum fusiforme fucoidan SP2 extends the lifespan of Drosophila melanogaster by upregulating the Nrf2-mediated antioxidant signaling pathway 2019, 2019, https://doi.org/10.1155/2019/ 8918914.
- [33] E. Deniaud-Bouët, K. Hardouin, P. Potin, et al., A review about brown algal cell walls and fucose-containing sulfated polysaccharides: cell wall context, biomedical properties and key research challenges, Carbohydr. Polym. 175 (2017) 395–408, https://doi.org/10.1016/j.carbpol.2017.07.082.
- [34] W. Jin, J. Wang, H. Jiang, et al., The neuroprotective activities of heteropolysaccharides extracted from Saccharina japonica, Carbohydr. Polym. 97 (2013) 116–120, https://doi.org/10.1016/j.carbpol.2013.04.055.
- [35] J. Wu, Y. Lv, X. Liu, et al., Structural study of sulfated fuco-oligosaccharide branched glucuronomannan from Kjellmaniella crassifolia by ESI-CID-MS/MS, J. Carbohydr. Chem. 34 (2015) 303–317, https://doi.org/10.1080/ 07328303.2015.1050593.
- [36] C. Nagy, E. Einwallner, Study of in vivo glucose metabolism in high-fat diet-fed mice using oral glucose tolerance test (OGTT) and insulin tolerance test (ITT), J. Vis. Exp. (2018), https://doi.org/10.3791/56672.
- [37] T. Minamisawa, J. Hirabayashi, Fragmentations of isomeric sulfated monosaccharides using electrospray ion trap mass spectrometry, Rapid Commun. Mass Spectrom. 19 (2005) 1788–1796, https://doi.org/10.1002/rcm.1985.
- [38] W. Jin, L. Ren, B. Liu, et al., Structural features of sulfated glucuronomannan oligosaccharides and their antioxidant activity, Mar. Drugs 16 (2018), https://doi. org/10.3390/md16090291.
- [39] W. Jin, X. He, J. Zhu, et al., Inhibition of glucuronomannan hexamer on the proliferation of lung cancer through binding with immunoglobulin G, Carbohydr. Polym. 248 (2020), 116785, https://doi.org/10.1016/j.carbpol.2020.116785.
- [40] Z. Fu, E.R. Gilbert, D. Liu, Regulation of insulin synthesis and secretion and pancreatic beta-cell dysfunction in diabetes, Curr. Diabetes Rev. 9 (2013) 25–53.
- [41] V.L. Tokarz, P.E. MacDonald, in: The cell biology of systemic insulin function 217, 2018, pp. 2273–2289, https://doi.org/10.1083/jcb.201802095.
- [42] N. Jeffery, L.W. Harries, β-cell differentiation status in type 2 diabetes, Diabetes Obes. Metab. 18 (2016) 1167–1175, https://doi.org/10.1111/dom.12778.
- [43] X. Li, T. Wan, Y. Li, Role of FoxO1 in regulating autophagy in type 2 diabetes mellitus (review), Exp. Ther. Med. 22 (2021) 707, https://doi.org/10.3892/ etm.2021.10139.
- [44] S. Tang, Y. Xin, M. Yang, et al., Osteoprotegerin promotes islet β cell proliferation in intrauterine growth retardation rats through the PI3K/AKT/FoxO1 pathway, Int. J. Clin. Exp. Pathol. 12 (2019) 2324–2338.
- [45] F. Cui, X. He, in: IGF-1 ameliorates streptozotocin-induced pancreatic β cell dysfunction and apoptosis via activating IRS1/PI3K/Akt/FOXO1 pathway 71, 2022, pp. 669–680, https://doi.org/10.1007/s00011-022-01557-3.
- [46] A. Hernandez-Segura, J. Nehme, M. Demaria, Hallmarks of cellular senescence, Trends Cell Biol. 28 (2018) 436–453, https://doi.org/10.1016/j.tcb.2018.02.001.
- [47] J.M. van Deursen, The role of senescent cells in ageing, Nature 509 (2014) 439–446, https://doi.org/10.1038/nature13193.
- [48] S.Y. Wang, P.A. Halban, J.W. Rowe, Effects of aging on insulin synthesis and secretion.Differential effects on preproinsulin messenger RNA levels, proinsulin biosynthesis, and secretion of newly made and preformed insulin in the rat, J. Clin. Invest. 81 (1988) 176–184, https://doi.org/10.1172/jci113291.
- [49] S. Lee, H.H. Dong, FoxO integration of insulin signaling with glucose and lipid metabolism, J. Endocrinol. 233 (2017) R67–r79, https://doi.org/10.1530/joe-17-0002
- [50] D. Accili, K.C. Arden, FoxOs at the crossroads of cellular metabolism, differentiation, and transformation, Cell 117 (2004) 421–426, https://doi.org/ 10.1016/s0092-8674(04)00452-0.
- [51] Y.I. Kitamura, T. Kitamura, J.P. Kruse, et al., FoxO1 protects against pancreatic beta cell failure through NeuroD and MafA induction, Cell Metab. 2 (2005) 153–163, https://doi.org/10.1016/j.cmet.2005.08.004.
- [52] X. Yu, Y.C. Long, H.M. Shen, Differential regulatory functions of three classes of phosphatidylinositol and phosphoinositide 3-kinases in autophagy, Autophagy 11 (2015) 1711–1728, https://doi.org/10.1080/15548627.2015.1043076.
- [53] D. Tang, Q.B. Chen, X.L. Xin, et al., Anti-diabetic effect of three new norditerpenoid alkaloids in vitro and potential mechanism via PI3K/Akt signaling pathway, Biomed. Pharmacother. 87 (2017) 145–152, https://doi.org/10.1016/j. biopha. 2016.12.058
- [54] L.M. Dickson, C.J. Rhodes, Pancreatic beta-cell growth and survival in the onset of type 2 diabetes: a role for protein kinase B in the Akt? Am. J. Physiol. Endocrinol. Metab. 287 (2004) E192–E198, https://doi.org/10.1152/ajpendo.00031.2004.
- [55] L. Elghazi, N. Balcazar, E. Bernal-Mizrachi, Emerging role of protein kinase B/Akt signaling in pancreatic beta-cell mass and function, Int. J. Biochem. Cell Biol. 38 (2006) 157–163, https://doi.org/10.1016/j.biocel.2005.08.017.

- [56] Y. Gao, G. Liao, C. Xiang, et al., Effects of phycocyanin on INS-1 pancreatic β-cell mediated by PI3K/Akt/FoxO1 signaling pathway, Int. J. Biol. Macromol. 83 (2016) 185–194, https://doi.org/10.1016/j.ijbiomac.2015.11.054.
 [57] H. Huang, D.J. Tindall, FOXO factors: a matter of life and death, Future Oncol. 2
- (2006) 83–89, https://doi.org/10.2217/14796694.2.1.83.
- [58] W. Wang, Y. Liu, Y. Chen, et al., Inhibition of Foxo1 mediates protective effects of ghrelin against lipotoxicity in MIN6 pancreatic beta-cells, Peptides 31 (2010) 307–314, https://doi.org/10.1016/j.peptides.2009.11.011.